Circulation

ORIGINAL RESEARCH ARTICLE

Natural Compound Library Screening Identifies New Molecules for the Treatment of Cardiac Fibrosis and Diastolic Dysfunction

BACKGROUND: Myocardial fibrosis is a hallmark of cardiac remodeling and functionally involved in heart failure development, a leading cause of deaths worldwide. Clinically, no therapeutic strategy is available that specifically attenuates maladaptive responses of cardiac fibroblasts, the effector cells of fibrosis in the heart. Therefore, our aim was to develop novel antifibrotic therapeutics based on naturally derived substance library screens for the treatment of cardiac fibrosis.

METHODS: Antifibrotic drug candidates were identified by functional screening of 480 chemically diverse natural compounds in primary human cardiac fibroblasts, subsequent validation, and mechanistic in vitro and in vivo studies. Hits were analyzed for dose-dependent inhibition of proliferation of human cardiac fibroblasts, modulation of apoptosis, and extracellular matrix expression. In vitro findings were confirmed in vivo with an angiotensin II–mediated murine model of cardiac fibrosis in both preventive and therapeutic settings, as well as in the Dahl salt-sensitive rat model. To investigate the mechanism underlying the antifibrotic potential of the lead compounds, treatment-dependent changes in the noncoding RNAome in primary human cardiac fibroblasts were analyzed by RNA deep sequencing.

RESULTS: High-throughput natural compound library screening identified 15 substances with antiproliferative effects in human cardiac fibroblasts. Using multiple in vitro fibrosis assays and stringent selection algorithms, we identified the steroid bufalin (from Chinese toad venom) and the alkaloid lycorine (from *Amaryllidaceae* species) to be effective antifibrotic molecules both in vitro and in vivo, leading to improvement in diastolic function in 2 hypertension-dependent rodent models of cardiac fibrosis. Administration at effective doses did not change plasma damage markers or the morphology of kidney and liver, providing the first toxicological safety data. Using next-generation sequencing, we identified the conserved microRNA 671-5p and downstream the antifibrotic selenoprotein P1 as common effectors of the antifibrotic compounds.

CONCLUSIONS: We identified the molecules bufalin and lycorine as drug candidates for therapeutic applications in cardiac fibrosis and diastolic dysfunction.

Katharina Schimmel, PhD*
Mira Jung, PhD*
Ariana Foinquinos, PhD*
et al

*Drs Schimmel, Jung, and Foinquinos contributed equally.

The full author list is available on p 765.

Key Words: diastole ■ fibrosis ■ hypertension ■ microRNAs

Sources of Funding, see page 766

https://www.ahajournals.org/journal/circ

Clinical Perspective

What Is New?

- Natural compound library screening in human cardiac fibroblasts identified novel compounds with antifibrotic properties.
- The compounds bufalin and lycorine show highly potent antifibrotic effects in vitro and in vivo and improve diastolic function in relevant models of heart failure.
- We provide evidence for cardioprotective, antifibrotic effects of the natural compounds bufalin and lycorine with a promising safety-tolerability profile, laying the groundwork for prospective preclinical and clinical studies with the aim of specifically treating cardiac fibrosis and diastolic dysfunction.

What Are the Clinical Implications?

- Although some state-of-the-art medications may improve fibrosis and diastolic dysfunction, no therapeutic strategy currently is available that is specifically designed to target fibroblasts, the effector cells of fibrosis in the heart.
- We provide strong evidence of natural compound–based preventive and therapeutic strategies against the development of cardiac fibrosis and diastolic dysfunction in clinically relevant models of heart failure.
- Preclinical and clinical development of specific cardiac antifibrotic molecules as presented here could lead to transformational changes in the treatment of patients with cardiac fibrosis and diastolic dysfunction.

In the healthy heart, extracellular matrix is essential to maintain both structure and integrity of the organ. In contrast, cardiac stress results in excessive production of extracellular matrix, leading to cardiac fibrosis.[1,2] Fibrosis subsequently triggers myocardial stiffness, ultimately impairing left ventricular (LV) diastolic and later systolic function.[3] Myocardial fibrosis favors progression to end-stage heart failure (HF), arrhythmias, and ischemia and therefore correlates with an increased mortality in patients, even under state-of-the-art treatment.[4] Thus, cardiac fibrosis constitutes not only a major determinant for the clinical outcome of patients with HF but also a therapeutic target of utmost interest and importance.

Thus, we applied a naturally derived substance library screen to search for novel antifibrotic, cardioprotective lead compounds for further development into new antifibrotic therapeutics. Subsequent refining strategies of functional in vitro and in vivo studies uncovered the cardiac glycoside bufalin and the alkaloid lycorine. Both molecules potently repressed the fibrotic response in human cardiac fibroblasts (HCFs), and both prevented and reversed fibrosis in cardiac fibrosis mouse models (implanted osmotic minipumps for systemic angiotensin II [Ang II] infusion). In addition, inhibition of cardiac fibrosis, along with improvement in diastolic performance, could be confirmed in the Dahl salt-sensitive rat model of HF with diastolic dysfunction. Previously, these 2 identified drug candidates were discovered to exhibit antitumor activities in preclinical studies.[5–16] Moreover, neuroprotective, anti-inflammatory, antiosteoporotic, and antimicrobial effects of the compounds have been described.[7,12,17–20] However, the application of bufalin or lycorine in the prevention or treatment of cardiac fibrosis and diastolic dysfunction has never been explored. In addition, their mode of action or influence on noncoding RNAs involved in cardiac fibrosis is unknown.

METHODS

Animal Experiments

All animal studies involving mice were performed in accordance with the relevant guidelines and regulations and with the approval of the Niedersächsisches Landesamt für Verbraucherschutz und Lebensmittelsicherheit (Germany), the Brigham and Women's Hospital, and the Ethical Committee for Animal Experimentation of the University of Navarra (Spain).

Statistical Analysis

All in vitro experiments were performed ≥3 independent times, as indicated in the figure captions, in duplicate, triplicate, or quadruplicate wells. The independent number of animals in each group is indicated in the figure legends. Data are displayed as mean of independent experiments/independent animal samples±SEM if not otherwise specified in the figure legend. Statistical analysis was carried out with the GraphPad Prism 6 software (GraphPad Prism Software Inc, San Diego, CA). For comparison of 2 groups, unpaired 2-tailed Student *t* test was applied, and for analysis of ≥3 groups, 1-way ANOVA with Turkey and 2-way ANOVA with Tukey multiple-comparisons test were performed if not otherwise specified in the figure legend. In all cases, a value of $P \leq 0.05$ was considered statistically significant.

A detailed Methods section is available in the online-only Data Supplement.

The data and analytical methods will be made available to other researchers for purposes of reproducing the results or replicating the procedure. Study materials can be provided only when a material transfer agreement is signed and if still available.

RESULTS

Natural Compound Screening Identifies Bufalin and Lycorine as Specific Antifibrotic Molecules in HCFs

Excessive accumulation of extracellular matrix in the diseased heart is caused by an increase in both proliferation rates and collagen production of cardiac fibroblasts. To uncover natural compounds suppressing

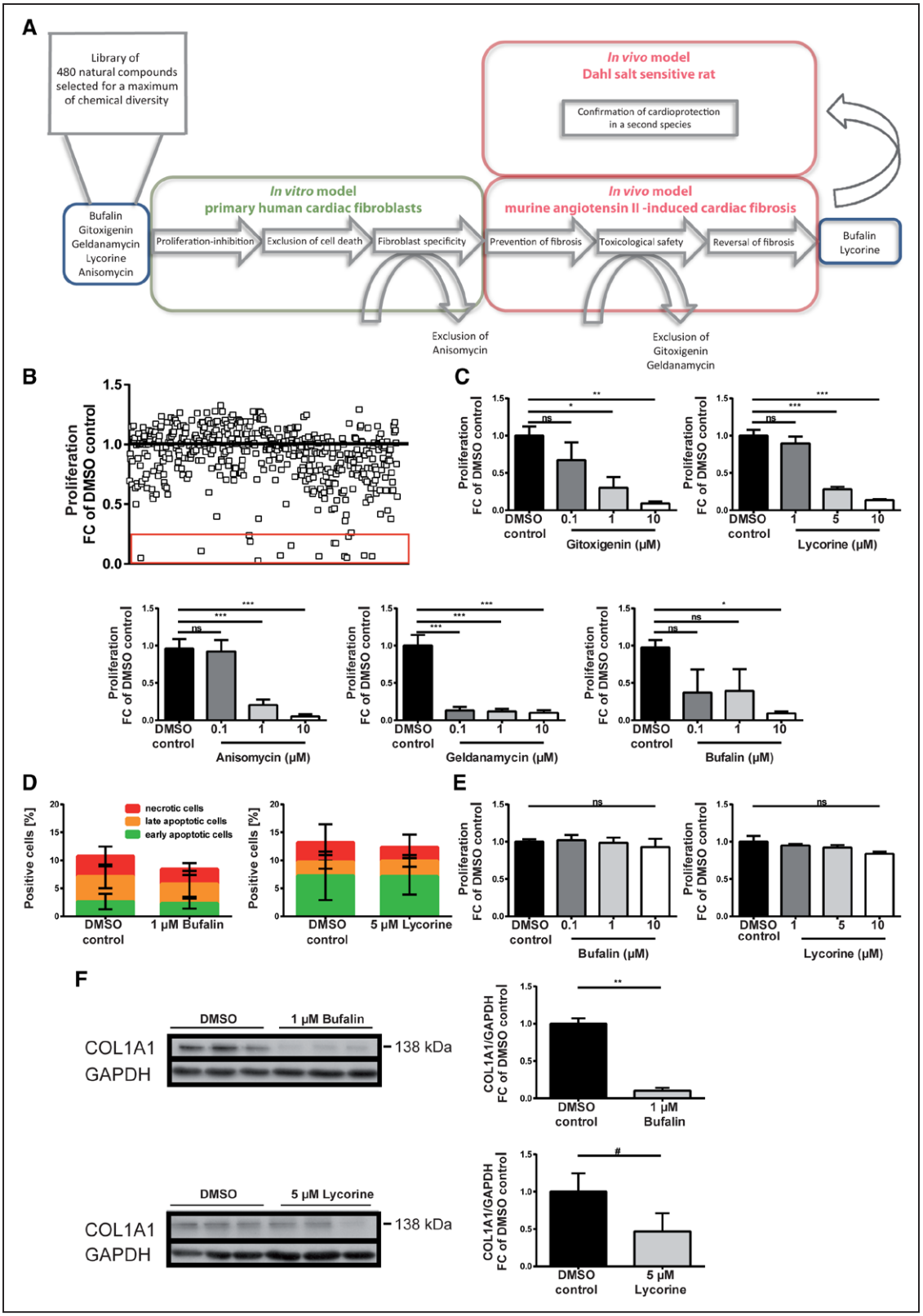

Figure 1. Bufalin and lycorine potently and specifically repress fibrotic responses in human cardiac fibroblasts (HCFs).
A, Filtering strategy, followed by in vitro and in vivo pipeline of analysis, uncovers antifibrotic lead compounds bufalin and lycorine. **B**, Functional screen of 480 naturally derived substances in vitro yielding natural compounds inhibiting the proliferation of HCFs. The cells were incubated for 24 hours as indicated, and proliferation of HCFs was measured by BrdU-ELISA. Fifteen candidates inhibiting the fibroblast proliferation fold change (FC) ≥75% are highlighted by the red rectangle. **C**, Dose-dependent inhibitory effects of bufalin, gitoxigenin, lycorine, anisomycin, and geldanamycin on proliferation of HCFs. The cells were incubated for 24 hours as indicated, and the proliferation of HCFs was measured by BrdU-ELISA (1-way ANOVA, Dunnett multiple-comparisons test, n=4-6). **D**, Positively validated hits do not induce cell death in HCFs. Cells were treated with respective compounds for 24 hours as indicated and (*Continued*)

fibrotic responses in cardiac fibroblasts, proliferation of HCFs was studied after incubation with 480 individual compounds, selected from a database comprising 150 000 natural products for a maximum of chemical diversity with the OptiSim algorithm (Figure 1A and 1B). Applying a selection threshold of fibroblast proliferation inhibition fold change ≥75%, we identified 15 candidates, of which 5 inhibited proliferation rates in a dose-dependent manner (Figure 1B and 1C). Next, we excluded cell death to be involved in the observed decrease in proliferation triggered by these compounds (bufalin, gitoxigenin, lycorine, anisomycin, and geldanamycin). Therefore, HCFs were treated with respective compounds using the effective doses and subjected to fluorescence-activated cell sorter analysis after annexin-7AAD staining (Figure 1D). To confirm fibroblast specificity of the remaining candidates, potential effects on proliferation rates of the cardiomyocyte cell line HL-1 were studied. As depicted in Figure 1A, except for anisomycine, all tested substances acted specifically on cardiac fibroblasts only, as evidenced by no impact on the proliferation of HL-1 cells (Figure 1E). On the basis of these selection criteria, the cardiac glycoside bufalin and the alkaloid lycorine were further assayed for suppression of collagen type I, α1 expression, the rigid and highly cross-linked extracellular matrix component produced in excess by activated fibroblasts. Treatment of HCFs with the 2 lead compounds, and in particular with bufalin, effectively decreased fibroblast collagen type I, α1 protein levels (Figure 1F). Likewise, collagen amounts secreted into the supernatant of HCFs were reduced by bufalin (Figure IA in the online-only Data Supplement).

To further elaborate on fibroblast-specific actions of bufalin and lycorine, we determined the cell size of neonatal rat cardiomyocytes stimulated with Ang II on treatment with the 2 lead drug candidates. Neither bufalin nor lycorine counteracted the hypertrophic growth of cardiomyocytes in vitro stimulated by Ang II (Figure IB and IC in the online-only Data Supplement). Of note, lycorine but not bufalin exerted slight inhibitory effects on proliferation of the rat renal fibroblast cell line NRK49F (Figure ID in the online-only Data Supplement). In contrast, bufalin in particular inhibited proliferation of primary human pulmonary fibroblasts (Figure IE in the online-only Data Supplement). These results might suggest a potential therapeutic implication of the substances not only in cardiac but also in renal or pulmonary fibrotic diseases, respectively.

Bufalin and Lycorine Prevent Fibrosis and Preserve Cardiac Function in Ang II–Induced Cardiac Remodeling

To verify whether the identified antifibrotic substances prevent fibrosis development at early stages also in vivo, C57BL/6N mice were infused with Ang II by subcutaneously implanted minipumps for 2 weeks. The natural substances (dissolved in dimethyl sulfoxide) or the solvent alone (as control) was injected intraperitoneally every other day until the end point, beginning 1 day after the start of Ang II infusion. Histological sections of the heart were studied for fibrosis development, and cardiac function was assessed both echocardiographically and hemodynamically. A schematic representation of the preventive in vivo study is depicted in Figure 2A. Ang II infusion led to a significant decrease in body weight (Figure IF in the online-only Data Supplement) which linked with increased ratios of heart to body weight in animals infused with the solvent only (controls); however, bufalin or lycorine did not significantly prevent this effect (Figure 2B). Treatment with bufalin significantly prevented cardiac fibrosis, as shown by a reduction of collagen deposition in histological sections of the hearts (Figure 2C). Lycorine showed also global antifibrotic effects, although this was of borderline significance (Figure 2C). However, further assessment of regional fibrosis measurements showed significant reductions in interstitial fibrosis and in perivascular fibrosis by treatment with bufalin. Treatment with lycorine also prominently decreased interstitial fibrosis; however, the significance of this effect was borderline (Figure IIA–IIC in the online-only Data Supplement).

Fibrosis development is associated with diastolic and eventually progression to systolic dysfunction in hypertensive mice, hereby closely recapitulating pathological remodeling common in fibrotic cardiac disease in humans. Thus, we evaluated mitral inflow and tissue Doppler signals to assess the effect of the compounds on diastolic function (Figure 2D). Echocardiographic evaluation of diastolic function revealed early signs of diastolic dysfunction with impaired relaxation after 2 weeks of Ang II treatment (Figure 2D through 2H) with decreased E/A ratio and increased deceleration time accompanied by slower peak mitral annular velocity, E′. Both compounds conferred improvements of relaxation, as evidenced by a decrease of the myocardial performance index (MPI) and the deceleration time, as well as rescued E/A ratios and E′. The increase of E′

Figure 1 Continued. subjected to fluorescence-activated cell sorter analysis after annexin-7AAD staining (unpaired *t* test, n=3). **E**, Dose-dependent inhibitory effects of bufalin and lycorine on proliferation of HCFs are fibroblast specific, as evidenced by no impact of the same concentrations of respective substances on the proliferation of the cardiomyocyte cell line HL-1. Cells were treated with the compounds for 24 hours as indicated, and proliferation of HL-1 cells was measured by BrdU-ELISA (1-way ANOVA, Dunnett multiple-comparisons test, n=3). **F**, Bufalin and, to a lesser extent, lycorine decrease expression levels of collagen type I, α1 (COL1A1) in HCFs shown in a representative Western blot. Cells were treated with respective substances for 24 hours as indicated, lysed, and analyzed for COL1A1 protein levels (normalized to GAPDH; unpaired *t* test). All values from **C** through **F** are presented as mean±SEM. DMSO indicates dimethyl sulfoxide; and ns, not significant. **P*<0.05, ***P*<0.01, ****P*<0.001, #*P*=0.265.

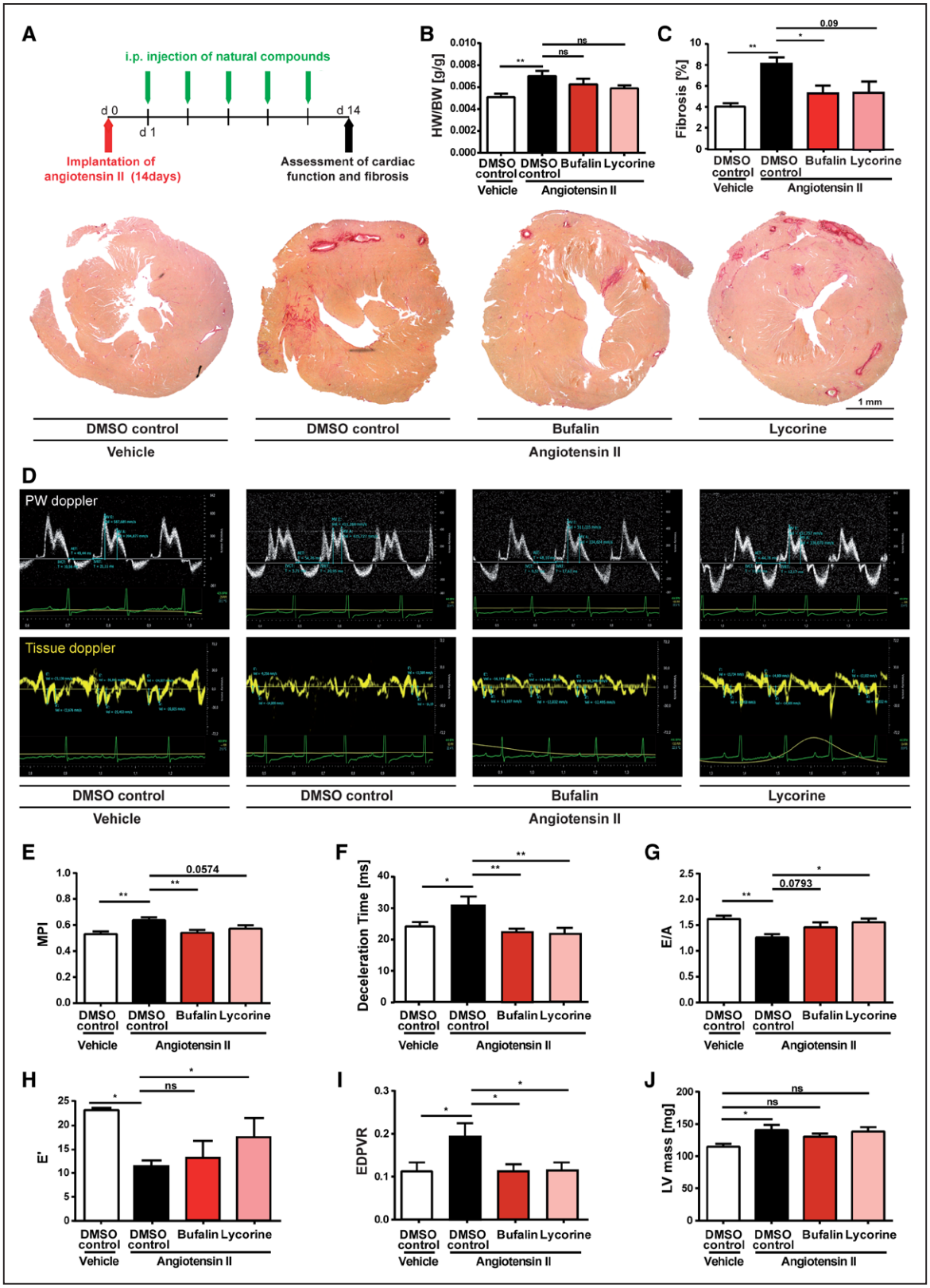

Figure 2. Bufalin and lycorine protect from angiotensin II (Ang II)–induced fibrotic cardiac disease in mice.

A, Schematic representation of the preventive in vivo study using a murine model of hypertensive heart disease. Diastolic dysfunction was induced in C57BL/6 mice via implantation of Ang II–filled minipumps, and bufalin or lycorine was injected intraperitoneally every other day during 2 consecutive weeks starting 1 day after the operation. Fourteen days after the operation, hearts were explanted for biochemical and histological analysis. **B**, Reduced heart-to-body weight ratios (HW/BW) on treatment as indicated compared with control animals (1-way ANOVA, Tukey multiple-comparisons test, n=14/17/17/14). **C**, Prevention of collagen deposition shown in representative images of cardiac histological sections of the whole heart and quantification of Picrosirius red–stained areas on administration of bufalin and lycorine (1-way ANOVA, Tukey multiple-comparisons test, n=10/11/10/11), scale bar=1 mm. (*Continued*)

indicates true improvement of tissue function, making pseudonormalization unlikely (Figure 2H). The preventive effect of lycorine on MPI and of bufalin on E/A ratio was of borderline significance (Figure 2D through 2G). Hemodynamic pressure-volume measurements were performed to assess LV compliance. Treatment with bufalin or lycorine completely counteracted the development of passive stiffness of the LV caused by the Ang II infusion, as evidenced by a reduction of the end-diastolic pressure-volume relationship (Figure 2I). In line with the heart weight data (Figure 2B), cardiac mass measured by echocardiography was slightly increased but unaffected by bufalin or lycorine in the Ang II–treated groups (Figure 2J).

Bufalin and lycorine were detectable in cardiac tissue (and plasma) of mice, confirming their uptake into the heart on systemic delivery (Figure IID and IIE in the online-only Data Supplement). Moreover, continuous monitoring of systolic and diastolic blood pressures in mice via telemetry showed that neither bufalin nor lycorine had any regulative impact on hypertension induced by Ang II, excluding the possibility that bufalin or lycorine confers cardioprotection by reducing elevated blood pressure (Figure IIF and IIG in the online-only Data Supplement). Of note, Ang II infusion for 8 weeks did not increase the number of terminal desoxynucleotidyl transferase–mediated dUTP-biotin nick-end labeling–stained cells in the myocardium, ruling out the possibility that bufalin or lycorine exerts cardioprotective effects by diminishing cardiomyocyte death (Figure IIH in the online-only Data Supplement). In line with this, the bcl-2–associated X protein/b-cell lymphoma 2 (BAX/BCL2) ratio based on mRNA levels in the same cardiac tissues remained comparable within all groups tested (Figure III in the online-only Data Supplement).

The anti-inflammatory effects of bufalin and lycorine have previously been described. In particular, attenuation of proinflammatory mediators such as tumor necrosis factor-α and interleukin (IL)-1β could be demonstrated.[19,21] Inflammation commonly precedes fibrosis development in cardiac diseases. We therefore measured mRNA levels of tumor necrosis factor-α and IL-1β in whole-heart tissues. Although trends toward lower transcriptional activities of tumor necrosis factor-α and IL-1β occurred on bufalin treatment, Ang II infusion did not lead to any significant activation of tumor necrosis factor-α or IL-1β expression (Figure IIJ and IIK in the online-only Data Supplement).

In terms of the safety and tolerability of the compounds, no signs of kidney and liver damage by plasma markers were found (Figure IIIA in the online-only Data Supplement). This provides the first promising data for further development of the 2 substances, bufalin and lycorine.

Bufalin and Lycorine Reverse Fibrosis and Recover Cardiac Function in Ang II–Induced Cardiac Remodeling

Our next aim was to test the beneficial effects of the identified antifibrotic compounds on cardiac fibrosis and function in a therapeutic setting, that is, when cardiac fibrosis was already established. Therefore, treatment of Ang II–infused mice with bufalin or lycorine was started at a time point when cardiac fibrosis and diastolic dysfunction were already evident. Bufalin, lycorine, or the solvent was injected intraperitoneally every other day for 6 consecutive weeks starting 2 weeks after start of the Ang II treatment (Figure 3A). Treatment with both compounds significantly reduced overall fibrosis in the myocardium (Figure 3B and Figure IIIB in the online-only Data Supplement) without affecting cardiomyocyte size (Figure IIIC and IIID in the online-only Data Supplement). The strong antifibrotic effect of both compounds is evidenced by detailed analysis of the perivascular and interstitial regions (Figure IVA through IVC in the online-only Data Supplement).

Hemodynamic and echocardiography assessment revealed the progression of diastolic dysfunction to a more severe stage, evidenced by enlarged left atria, reduced dP/dtmin, statistically significant increase of tau and end-diastolic pressure-volume relationship, increased E/A ratio, highly increased MPI and peak E/E', and decreased deceleration time (Figure 3D through 3H, Figure IVD and IVE in the online-only Data Supplement, and Table 1). Both compounds were able to partly reverse diastolic dysfunction; bufalin recovered hemodynamic parameters (dP/dtmin, tau, and end-diastolic pressure-volume relationship) and both MPI and deceleration time (Figure 3C through 3E and Figure IVE in the online-only Data Supplement); and lycorine showed protective effects on diastolic dysfunction to a lesser degree with borderline significance (Figure 3D and 3E). Both compounds reduced the elevated E/A ratio and the left atrial area (Figure 3F and Table 1), and tissue Doppler imaging confirmed faster tissue motion

Figure 2 Continued. **D**, Isovolumic contraction time, isovolumic relaxation time, aortic ejection time, and E and A waves are measured by pulsed-wave (PW) Doppler from the apical 4-chamber view from the lateral mitral valve (**top**). Early (E') and atrial (A') peak velocities are measured from tissue Doppler signal at the mitral annulus (**bottom**). Preservation of myocardial performance index (MPI; **E**; 1-way ANOVA, Tukey multiple-comparisons test, n=11/21/16/12), deceleration time (**F**; 1-way ANOVA, Tukey multiple-comparisons test, n=11/21/16/12), improvement of peak E/A ratio (**G**; 1-way ANOVA, Tukey multiple-comparisons test, n=8/16/11/7), and improved E' peak value (**H**; 1-way ANOVA, Tukey multiple-comparisons test, n=8/16/11/7) after treatment with compounds as indicated. **I**, Preservation of left ventricular (LV) compliance by bufalin or lycorine, assessed by end-diastolic pressure-volume relationship (EDPVR) obtained by linear fits of the EDPVR slope, resulting from the shift of pressure-volume loops after transient vena cava occlusions (1-way ANOVA, Tukey multiple-comparisons test, n=8/9/6/8). **J**, Significant increase in LV mass by Ang II infusion in animals treated with the solvent only (controls) but not in mice treated with bufalin or lycorine (1-way ANOVA, Tukey multiple-comparisons test, n=8/11/9/9). All values from **B** through **J** are presented as mean±SEM. DMSO indicates dimethyl sulfoxide. *P<0.05. **P<0.01.

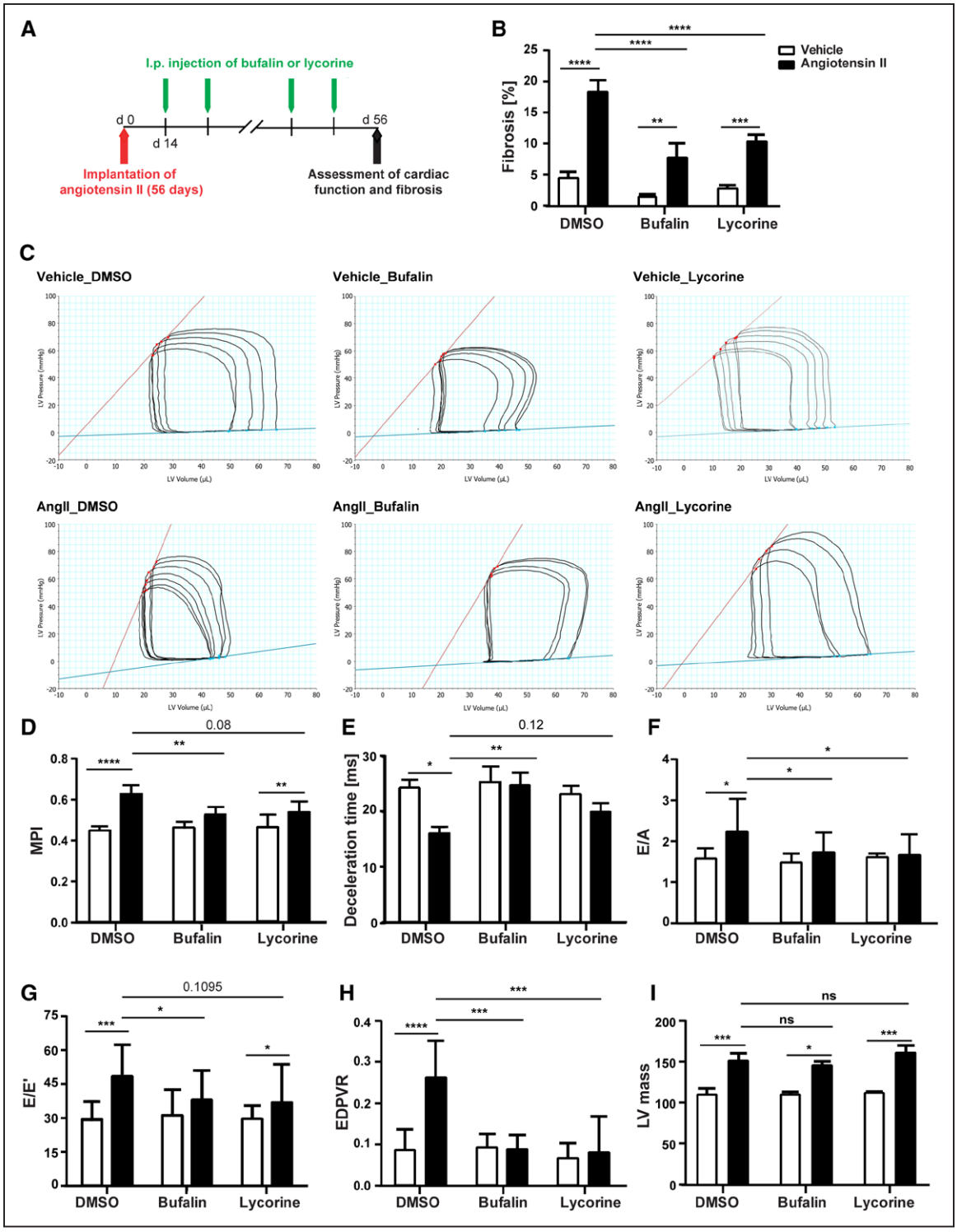

Figure 3. Bufalin and lycorine reverse established fibrosis and improve heart function in hypertensive mice.
A, Therapeutic in vivo study using a murine model of systemic hypertension. Bufalin, lycorine, or dimethyl sulfoxide (DMSO) was injected intraperitoneally every other day for 6 consecutive weeks starting 2 weeks after the implantation of minipumps filled with angiotensin II (Ang II). **B**, Significant amelioration of cardiac fibrosis in established diastolic heart failure on treatment with bufalin and lycorine by 50% (2-way ANOVA, Tukey multiple-comparisons test, n=19/8/7/17/18/16). **C**, Representative images of hemodynamic pressure-volume loops. Both compounds were able to partly reverse diastolic dysfunction; bufalin recovered hemodynamic parameters (dP/dtmin, tau, and end-diastolic pressure-volume relationship [EDPVR]) compared with the Ang II group. **D** through **F**, Strong trend of reduction of myocardial performance index (MPI; 1-way ANOVA, n=19/8/7/17/18/16) and prolongation of deceleration time (2-way ANOVA, Tukey multiple-comparisons test, n=19/8/7/17/18/16) by the lead compounds and decreased peak E/A (2-way ANOVA, Tukey multiple-comparisons test, n=18/8/7/14/15/15) on treatment with compounds. **G**, Strong trend in reduction of peak E/E' on treatment with both bufalin and lycorine (2-way ANOVA, Tukey multiple-comparisons test, n=14/8/7/14/14/15). **H**, Significant improvement of load-independent EDPVR by bufalin and lycorine on systemic hypertension (2-way ANOVA, Tukey multiple-comparisons test, n=14/8/7/14/14/15). **I**, Significant increase in left ventricular (LV) mass by Ang II infusion in animals treated (*Continued*)

during diastole on treatment with bufalin as represented by recovery of E/E' ratios in Ang II–treated mice (Figure 3G, Figure IVE in the online-only Data Supplement, and Table 1). Moreover, 2D speckle-tracking strain echocardiography uncovered a significant reversal of the downshift of both radial and longitudinal strains (percent) in the base, middle, and apical regions of the heart triggered by Ang II infusion on treatment with bufalin and lycorine (Table 2 and Figure IVF through IVH in the online-only Data Supplement). Pressure-volume analysis revealed that bufalin and lycorine improved LV compliance, as evidenced by a significant reduction of end-diastolic pressure-volume relationship, a load-independent parameter of LV stiffness (Figure 3H), without affecting end-systolic pressure-volume relationship (Figure IVD in the online-only Data Supplement). Thus, systematic assessment of cardiac function unveiled a prominent reduction of passive stiffness of the LV on systemic hypertension by the antifibrotic activity of the lead compounds (especially in the therapeutic setup, eg, a situation in which treatment started only after fibrosis and diastolic dysfunction were already established). Ang II infusion significantly increased LV mass in animals infused with the solvent only (controls), which remained unchanged in mice treated with bufalin or lycorine (Figure 3I). There was no difference between treatments within the control groups (bufalin or lycorine only versus vehicle only groups), indicating that the compounds are without cardiac effects under basal conditions (Figure 3B through 3I).

To provide first insight into safety and tolerability also after the prolonged administration of the substances (6 weeks), changes in the morphology, fibrosis, necrosis, and inflammation of kidney and liver were evaluated (Figure VA in the online-only Data Supplement).

Ang II infusion for 8 weeks (Figure VB in the online-only Data Supplement) led to a less pronounced induction of fibrosis in female mice, which was, however, also ameliorated by the 2 lead compounds (Figure VC in the online-only Data Supplement). In line with this finding, MPI remained almost unchanged among the groups tested (Figure VD in the online-only Data Supplement). In contrast, Ang II infusion significantly increased isovolumic relaxation time/aortic ejection time in female mice infused with the solvent only (controls), which could be attenuated in animals treated with bufalin or lycorine (Figure VE in the online-only Data Supplement). The reduced responsiveness of female animals to Ang II infusion compared with age-matched male mice is likely caused by the presence of estrogen in females; the protective effects of estrogen (hypertension and cardiovascular disease) are well established.[22,23]

Collectively, these data emphasize amelioration of cardiac function and fibrosis in the diseased heart in a therapeutic setting. This may open up novel opportunities for the future treatment of patients with established cardiac fibrosis and diastolic dysfunction.

Lycorine and Bufalin Prevent the Development of Cardiac Fibrosis and Diastolic Dysfunction in Hypertensive Rats

Hypertension is one of the major causes for the development of HF with diastolic dysfunction. These patients typically exhibit heterogeneous histories of conglomerate risk factors such as diabetes mellitus, dyslipidemia, obesity, atrial fibrillation, aging, or renal dysfunction.[24] The Dahl salt-sensitive rat fed a high-salt diet represents the most frequently used model of systemic hypertension–induced HF with diastolic dysfunction, developing common comorbidities such as dyslipidemia and renal failure.[25] Moreover, the close reproduction of the human cardiac pathophysiology further strengthens clinical relevance and thus was used as a supplementary model to test the efficacy of both antifibrotic compounds (Figure 4A). Remarkably, evaluation of the hearts revealed that fibrosis development was prevented by both bufalin and lycorine in rats fed a high-salt diet. This was evident by near-normal values of collagen volume fraction, collagen cross-linking, and collagen deposition in whole-heart sections of treated rats (Figure 4B through 4D). Both bufalin and lycorine showed no significant impact on cardiomyocyte size in the Dahl salt-sensitive rat model (Figure 4E). Collectively, these results imply beneficial fibroblast-specific actions of bufalin and lycorine. As expected, echocardiographic evaluation of cardiac function revealed progressive diastolic dysfunction in rats fed a high-salt diet, evidenced by the reversed hemodynamic parameters tau and dP/dtmin (borderline significance) and an increased E/A ratio. Both compounds improved diastolic properties, as reflected by significant reductions of MPI, isovolumic relaxation time/aortic ejection time, and E/A and peak E/E' ratios compared with control rats fed a high-salt diet (Figure 4F through 4I, Table 3, and Figure VIA in the online-only Data Supplement).

Treatment with both compounds had no impact on renal inflammation, tubular injury, loss of brush border, protein- and detritus-containing casts, thrombotic microangiopathy, glomerulosclerosis, or arteriosclerosis or arteriolosclerosis induced in kidneys by the high-salt diet in hypertensive rats (Figure VIB in the online-only Data Supplement). Likewise, livers of the hypertensive rats showed loss of glycogen and steatosis independently of compound treatment. In addition, vessel wall

Figure 3 Continued. with the solvent only (controls) but not in mice treated with bufalin or lycorine (2-way ANOVA, Tukey multiple-comparisons test, n=19/8/7/16/17/16). All values from **B** through **I** are presented as mean±SEM. ESPVR indicates end-systolic pressure-volume relationship; and ns, not significant. **P*<0.05, ***P*<0.01, ****P*<0.001, *****P*<0.0001.

Table 1. Echocardiographic and Hemodynamic Parameters of the Therapeutic Approach in an Ang II–Infused Mouse Model

	Vehicle Group			Ang II Group		
	DMSO	Bufalin	Lycorine	DMSO	Bufalin	Lycorine
Echocardiographic parameters						
Heart rate, bpm	458±38.56	460±59.64	426.8±29.38	455.8±55.64	440.1±41.56	450.9±42.35
LVEDV, mL	75.21±9.54	71.83±9.91	71.41±9.19	69.52±26.74	79.98±33.06	75.30±28.13
LVESV, mL	25.26±10.65	33.29±15.96	31.51±5.01	33.49±21.11	41.74±30.16	40.49±24.33
EF, %	67.93±12.25	62.60±10.65	57.38±5.90	58.80±15.70	57.10±14.07	55.58±14.35
EDD, mm	3.94±0.30	4.05±0.21	4.03±0.22	3.87±0.65	4.14±0.75	4.07±0.60
ESD, mm	2.39±0.59	2.87±0.54	2.87±0.19	2.83±0.66*	3.03±0.96	3.05±0.82
FS, %	36.20±6.61	31.63±7.28	31.70±3.32	30.80±11.92	29.93±9.60	28.97±9.97
Peak E, cm/s	655±88.68	612.73±112.41	643±78.42	588.9±126.6	569.3±113	550.6±148.31
Peak A, cm/s	453.9±95.06	444.11±107.99	415.12±61.60	306.7±91.3*	364.04±100.08†	328.6±99.50
E/A ratio	1.48±0.24	1.41±0.25	1.56±0.11	2.15±0.85*	1.64±0.53(0.08)	1.57±0.56†
E', cm/s	20.35±6.48	20.53±3.97	21.65±2.44	13.10±3.12*	16.05±4.26†	14.14±2.69
A', cm/s	16.08±3.31	16.56±4.99	18.59±2.35	17.56±5.61	12.65±3.56†	12.12±3.71†
IVRT, ms	14.13±2.47	13.07±2.26	12.93±5.11	11.67±3.91*	16.12±4.11†	14.62±4.85(0.06)
IVCT, ms	9.23±3.27	10.46±2.95	11.01±4.78	13.77±3.57*	9.56±3.35†	11.02±3.07†
LVET, ms	53.83±5.09	52.34±3.69	55.10±6.36	43.67±4.21*	50.00±7.77†	48.12±6.97(0.06)
LAd, mm	1.93±0.20	1.71±0.34	1.91±0.09	2.15±0.69	1.85±0.45	1.73±0.47
LAs, mm	0.64±0.23	0.54±0.16	0.64±0.15	1.22±0.46*	0.74±0.11(0.08)	1.05±0.63
Millar parameters						
Heart rate, bpm	453.8±36.07	437.3±20.94	419.9±24.45	415.1±32.85	425.1±52.64	468.3±24.33
EDPVR	0.087±0.05	0.090±0.03	0.066±0.03	0.26±0.09*	0.087±0.03†	0.084±0.08†
ESPVR	2.01±0.60	3.89±2.11	1.84±0.66	3.08±1.5	2.91±1.48	4.35±2.12
Ees/Ea	1.19±0.36	1.99±1.22	1.03±0.26	1.14±0.49	1.39±0.73	1.28±0.74
dP/dtmax, mm Hg/s	6175±1498	5674±1608	5369±1601	5488±688.7	5549±1271	6167±1552
dP/dtmin,mm Hg/s	−6910±1618	−6174±1770	−6459±1383	−5527±961.6(0.07)	-5547±1890	-5689±1530
Tau, ms	6.25±0.71	7.18±1.20	7.41±0.87	7.78±1.81*	7.52±1.51	7.64±1.56
SV, mL	41.46±4.86	36.03±7.31	40.54±6.02	30.8±9.47*	39.55±7.41(0.06)	28.58±7.76
EF, %	57.12±6.28	57.55±17.67	60.69±6.32	45.55±14.43	43.5±11.41	43.53±19.47

Data are expressed as mean±SD. Two-way ANOVA, Tukey multiple-comparisons test. Ang II indicates angiotensin II; dP/dtmax, point of maximum pressure increase; dP/dtmin, point of maximum pressure decrease; Ea, arterial elastance; EDD, end diastolic diameter; EDPVR, end-diastolic pressure-volume relationship; EF, ejection fraction; ESD, end systolic diameter; ESPVR, end-systolic pressure-volume relationship; FS, fractional shortening; IVCT, isovolumetric contraction time; IVRT, isovolumetric relaxation time; LAd, left atrial diastolic size; LAs, left atrial systolic size; LVEDV, left ventricular end-diastolic volume; LVESV, left ventricular end-systolic volume; LVET, left ventricular ejection time; SV, stroke volume; and tau (Weiss), time constant of active relaxation.

*Comparison between vehicle-treated and Ang II–treated mice, $P<0.05$.

†Effect of compounds in Ang II–treated mice, $P<0.05$).

necrosis and thrombotic microangiopathy were evident only in hypertensive animals that did not receive lycorine (Figure VIC in the online-only Data Supplement). Again, both compounds showed no effect on heart weight or lung weights (Figure VID and VIE in the online-only Data Supplement). Lung water content also was not changed among groups (data not shown). Weekly dietary food intake was not affected by lead compound injections (Figure VIF in the online-only Data Supplement), excluding the possibility that the protective effects are being influenced by factors related to high-salt diet consumption.

Profibrotic MicroRNA 671-5p Is a Common Effector of the Identified Antifibrotic Naturally Derived Substances

To elucidate a potential influence of the identified natural substances on endogenous microRNAs (miRNAs), key posttranscriptional regulators of gene expression, miRNA deep sequencing in primary HCFs was performed. Levels of the highly conserved miR-671-5p were consistently and significantly reduced after treatment of primary HCFs with all 5 antifibrotic lead compounds from the initial screen in vitro (Figure 5A and 5B). This result suggested that miR-671-5p might play

Table 2. Global Strain Analysis of 6 Cardiac Segments of the Therapeutic Approach in Ang II–Infused Mouse Model

	Vehicle			Ang II		
	DMSO	Bufalin	Lycorine	DMSO	Bufalin	Lycorine
RS, %						
Seg 1	39.98±19.28	44.77±14.55	39.55±13.34	14.78±14.33	28.51±23.85	28.89±14.76
Seg 2	48.49±11.89	35.28±12.58	31.67±9.10	23.87±7.37	28.66±12.13	34.13±14.57
Seg 3	29.51±12.42	24.38±16.29	28.80±9.40	19.52±11.29	22.83±5.75	24.50±13.96
Seg 4	41.42±17.66	50.60±21.74	35.38±7.53	31.41±14.77	33.07±12.53	31.84±16.40
Seg 5	48.76±19.91	49.27±20.17	44.20±6.682	32.19±10.67	31.43±11.20	38.08±17.70
Seg 6	34.53±17.60	32.51±23.02	27.32±9.81	20.19±9.14	30.73±13.94	30.37±11.98
LS, %						
Seg 1	−19.45±12.80	−16.33±5.99	−13.75±5.92	−7.17±5.92	−10.75±12.02	−10.75±7.53
Seg 2	−16.42±11.17	−12.94±11.34	−14.69±2.99	−14.39±5.99	−13.03±6.01	−13.67±8.74
Seg 3	−24.36±10.74	−30.48±7.21	−21.34±3.86	−15.18±10.69	−27.14±9.16	−15.50±8.04
Seg 4	−11.05±11,08	−10.12±11.59	−12.79±3.92	−9.96±5.92	−7.96±5.75	−10.63±6.26
Seg 5	−15.59±4.57	−15.66±1.05	−16.13±6.85	−12.80±3.77	−17.34±6.32	−19.09±5.77
Seg 6	−19.71±4.58	−20.12±11.67	−15.31±3.47	−15.96±5.25	−17.61±5.11	−12.13±6.61

Data are expressed as mean±SD. Ang II indicates angiotensin II; DMSO, dimethyl sulfoxide; LS, longitudinal strain; RS, radial strain; Seg 1, posterior base; Seg 2, posterior mid; Seg 3, posterior apex; Seg 4, anterior base; Seg 5, anterior mid; and Seg 6, anterior apex.

a key role in the fibrotic response. Indeed, miR-671-5p regulated both fibrosis and inflammatory pathways in HCFs. Specific overexpression of miR-671-5 in HCFs led to transcriptional activation of α-smooth muscle actin (α-SMA), connective tissue growth factor, and the pro-inflammatory cytokines IL-6 and IL-8, indicating that miR-671-5p is sufficient to induce fibrotic and inflammatory responses in vitro (Figure 5C and Figure VIIA in the online-only Data Supplement). To delineate the mechanistic involvement of miR-671-5p in a cellular antifibrotic pathway activated by bufalin, the impact of miR-671-5p overexpression on transcriptional activation of α-SMA of primary HCFs on treatment with bufalin was monitored. Bufalin treatment decreased α-SMA expression in primary HCFs transfected with miR-mimic control or miR-671-5p compared with dimethyl sulfoxide control. Antifibrotic effects of bufalin on α-SMA expression of primary HCFs are significantly disturbed on overexpression of miR-671-5p, reflected by elevated α-SMA expression (Figure 5D), suggesting a role for miR-671-5p in the antifibrotic efficacy of bufalin.

Because of an intronic localization of miR-671-5p, expression of its host gene chondroitin polymerizing factor (*CHPF*) was additionally determined in primary HCFs after treatment with the lead compounds. Expression levels of *CHPF*, however, did not change consistently in primary HCFs on treatment with the identified molecules (Figure VIIB in the online-only Data Supplement), suggesting that the substances do not directly drive transcription of the miR-671-5p host gene *CHPF*.

Consistently, increased miR-671-5p expression could be observed in fibrotic conditions in vivo. Cardiac stress was induced in wild-type mice via infusion of Ang II. Indeed, cell fractionation experiments using hearts of mice after implantation of minipumps filled with Ang II or vehicle showed a significant and fibroblast-specific activation of miR-671-5p (Figure 5E). This activation was found to be counteracted by bufalin, confirming a possible functional importance of this miRNA in the antifibrotic action of bufalin in vivo (Figure VIIC in the online-only Data Supplement).

In summary, highly conserved miR-671-5p (according to miRBase, http://www.mirbase.org) was determined as a common effector of the lead compounds and as a key player of the fibrotic response in HCFs in vitro. Moreover, our studies underscore a functional role of miR-671-5p in fibrosis development in vivo and highlight its potential clinical importance.

Antifibrotic Selenoprotein P1 Is a Target of miR-671-5p in Cardiac Fibroblasts

Bioinformatic analysis using TargetScanHuman (version 7.1) predicted an 8mer miR-671-5p binding site in the 3′ untranslated region of selenoprotein P1 (*SEPP1*) that is conserved also in the murine species (Figure 6A). The cardioprotective role of the dietary trace element selenium has been shown in a plethora of cardiac stress conditions ranging from myocardial hypertrophy to diabetes mellitus– and metabolic syndrome–induced cardiac stress, ischemia/reperfusion, homocysteine dysregulation, and doxorubicin toxicity and is dependent on its incorporation into selenoproteins.[26–28] In line with this finding, effective silencing of *SEPP1* in HCFs via siRNA chemistry led to enhanced collagen type I, α1 expression in HCFs (Figure VIIE and VIIF in the

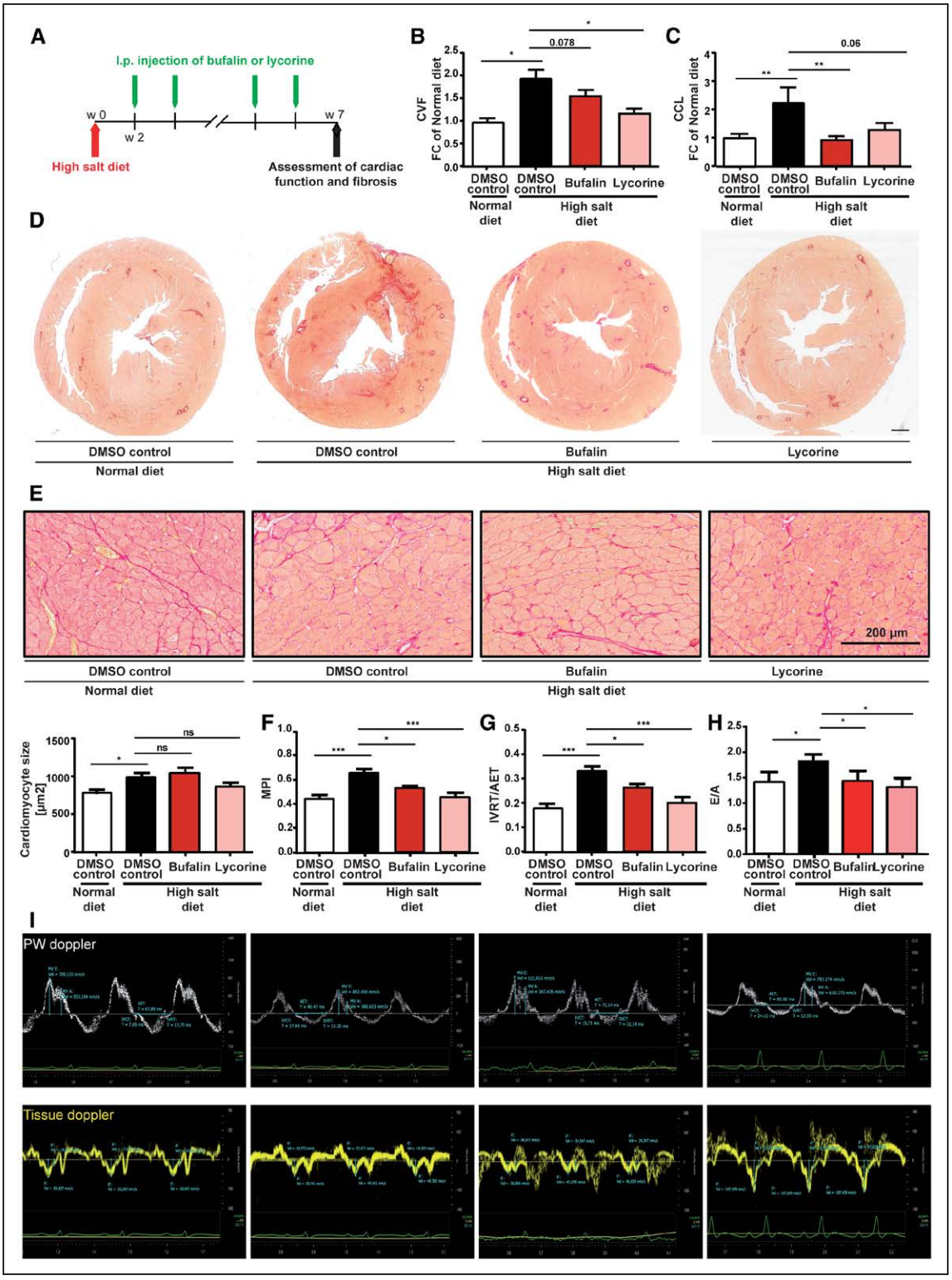

Figure 4. Lycorine and bufalin diminish fibrosis, diastolic dysfunction, and pulmonary congestion in the Dahls salt-sensitive rat.
A, In vivo study using a model of hypertension-induced diastolic dysfunction. Lycorine, bufalin, or dimethyl sulfoxide (DMSO) was injected intraperitoneally every other day for 5 consecutive weeks starting 2 weeks after induction of hypertension by a high-salt diet. **B** through **D**, Effective and significant reduction of collagen volume fraction (CVF; 1-way ANOVA, Tukey multiple-comparisons test, n=17/16/10/13), collagen cross-linking (CCL; 1-way ANOVA, Tukey multiple comparisons test, n=17/16/10/13), and collagen accumulation in the myocardium as shown in representative images of Picrosirius red staining; scale bar=1 mm. **E**, No significant impact on cardiomyocyte area shown in representative images and corresponding quantification of heart sections (1-way ANOVA, Tukey multiple-comparisons test, n=17/16/10/13); scale bar=200 µm. **F** through **H**, Significantly ameliorated myocardial performance index (MPI) and isovolumic relaxation time/aortic ejection time (IVRT/AET) in compound-treated rats compared with rats fed a high-salt diet (1-way ANOVA, Tukey multiple-comparisons test, n=10/9/10/13), as well as significant reduction of peak E/A (1-way ANOVA, Tukey multiple-comparisons test, n=10/9/10/13) on treatment with lycorine but not with bufalin. **I**, Representative pulsed-wave (PW) Doppler and tissue Doppler images from each group. All values from **B**, **C**, and **E** through **H** are presented as mean±SEM. **P*<0.05, ***P*<0.01, ****P*<0.001.

Table 3. Echocardiographic and Hemodynamic Parameters of the Therapeutic Study Done in the High-Salt Diet–Induced Rat Model

	Normal Diet	High-Salt Diet		
	DMSO	DMSO	Bufalin	Lycorine
Echocardiographic parameters				
Heart rate, bpm	395.4±26.46	368.7±40.85	363.8±26.1	388.3±34.43
LVEDV, mL	269.9±33.8	299.6±56.78	300.8±49.52	320.5±45.95
LVESV, mL	44.88±11.33	80.33±28.97*	89.19±37.43	76.49±13.39
EF, %	83.15±5.04	72.36±6.14*	70.38±12.20	76.07±3.57
EDD, mm	7.16±0.39	7.36±0.68	7.50±0.56	7.73±0.51
ESD, mm	3.30±0.349	4.19±0.61*	4.34±0.83	4.14±0.33
FS, %	53.85±5.58	43.07±5.41*	42.15±10.28	46.44±3.36
Peak E, cm/s	846±151.6	870.5±113.4	904.1±241.2	889.3±133.1
Peak A, cm/s	603.8±96.89	552.3±120.8	640.7±181.5	623.9±108.2
E/A ratio	1.40±0.19	1.83±0.16*	1.43±0.18†	1.31±0.23†
E′, cm/s	−47.34±16.46	−44.25±29.76	−49.85±26.89	−62±24.85
A′, cm/s	−46.52±24.83	−49.54±10.39	−46.46±12.81	−49.94±24.05
IVRT, ms	11.56±2.69	20.74±3.60*	17.52±3.26(0.09)	13.93±2.22†
IVCT, ms	16.3±3.66	21.25±3.57*	18.29±1.91(0.06)	17.32±3.84(0.06)
LVET, ms	61.95±4.38	62.83±3.22	66.23±3.58(0.08)	68.23±7.30(0.09)
Millar parameters				
Heart rate, bpm	346.1±21.65	349.7±22.12	345.1±20.47	362±37.51
EDPVR, mm Hg/μL	0.054±0.036	0.068±0.099	0.048±0.021	0.055±0.032
ESPVR, mm Hg/μL	0.89±0.07	1.51±0.66	0.91±0.47	1.03±0.52
Ees/Ea	1.77±0.21	2.40±1.03	1.39±0.85	1.73±1.06
dP/dtmax, mm Hg/s	6890±1203	5912±537.9(0.07)	6130±647.3	7510±951.4†
dP/dtmin, mm Hg/s	−8965±1674	−7900±1210(0.09)	−8426±1164	−9613±2616(0.100)
Tau, ms	8.90±1.03	10.06±0.98(0.06)	9.96±1.29	9.20±0.76(0.07)
SV, mL	228.5±46.97	176±33.52(0.09)	186.1±35.28	216±50.28
EF, %	92.92±8.46	73.29±10.58*	74.17±13.43	82.97±14.85

Data are expressed as mean±SD. Two-way ANOVA, Tukey multiple-comparisons test. DMSO indicates dimethyl sulfoxide; dP/dtmax, point of maximum pressure increase; dP/dtmin, point of maximum pressure decrease; Ea, arterial elastance; EDD, end-diastolic diameter; EDPVR, end-diastolic pressure-volume relationship; EF, ejection fraction; ESD, end-systolic diameter; ESPVR, end-systolic pressure-volume relationship; FS, fractional shortening; IVCT, isovolumetric contraction time; IVRT, isovolumetric relaxation time; LAd, left atrial diastolic size; LAs, left atrial systolic size; LVEDV, left ventricular end-diastolic volume; LVESV, left ventricular end-systolic volume; LVET, left ventricular ejection time; SV, stroke volume; and tau, time constant of active relaxation.

*Comparison of DMSO control between normal diet and high-salt-diet rats, $P<0.05$.

†Effect of compounds in high-salt-diet rats, $P<0.05$.

online-only Data Supplement). Repression of *SEPP1* by miRNA-671-5p would therefore support the detrimental activity of this miRNA. To validate the bioinformatic prediction via TargetScanHuman, we cloned the 3′ untranslated region of *SEPP1* downstream of the firefly luciferase gene and found the normalized luciferase activity to be markedly reduced on cotransfection of the construct with miR-671-5p mimic compared with the miR-mimic control (Figure 6B). To prove that *SEPP1* is a target of miR-671-5p in primary HCFs, *SEPP1* levels on overexpression of miR-671-5p were monitored. Levels of *SEPP1* were prominently and significantly decreased in primary HCFs after overexpression of miR-671-5p (Figure 6C). These data validate *SEPP1* as a target of miR-671-5p in primary HCFs. *SEPP1* levels were found to be increased (whereas miR-671-5p levels were decreased) in primary HCFs after treatment with the lead antifibrotic substances, particularly geldanamycin and bufalin (Figure 6D). These results suggest a protective role of *SEPP1*, possibly preventing myocardial stiffness in vivo. We consistently found that expression levels of *SEPP1* decreased in fibrotic cardiac tissue of mice infused with Ang II for 8 weeks. Ang II–induced decline of *SEPP1* mRNA was effectively recovered by treatment with the lead compounds over a time period of 6 weeks. However, no effect on *SEPP1*

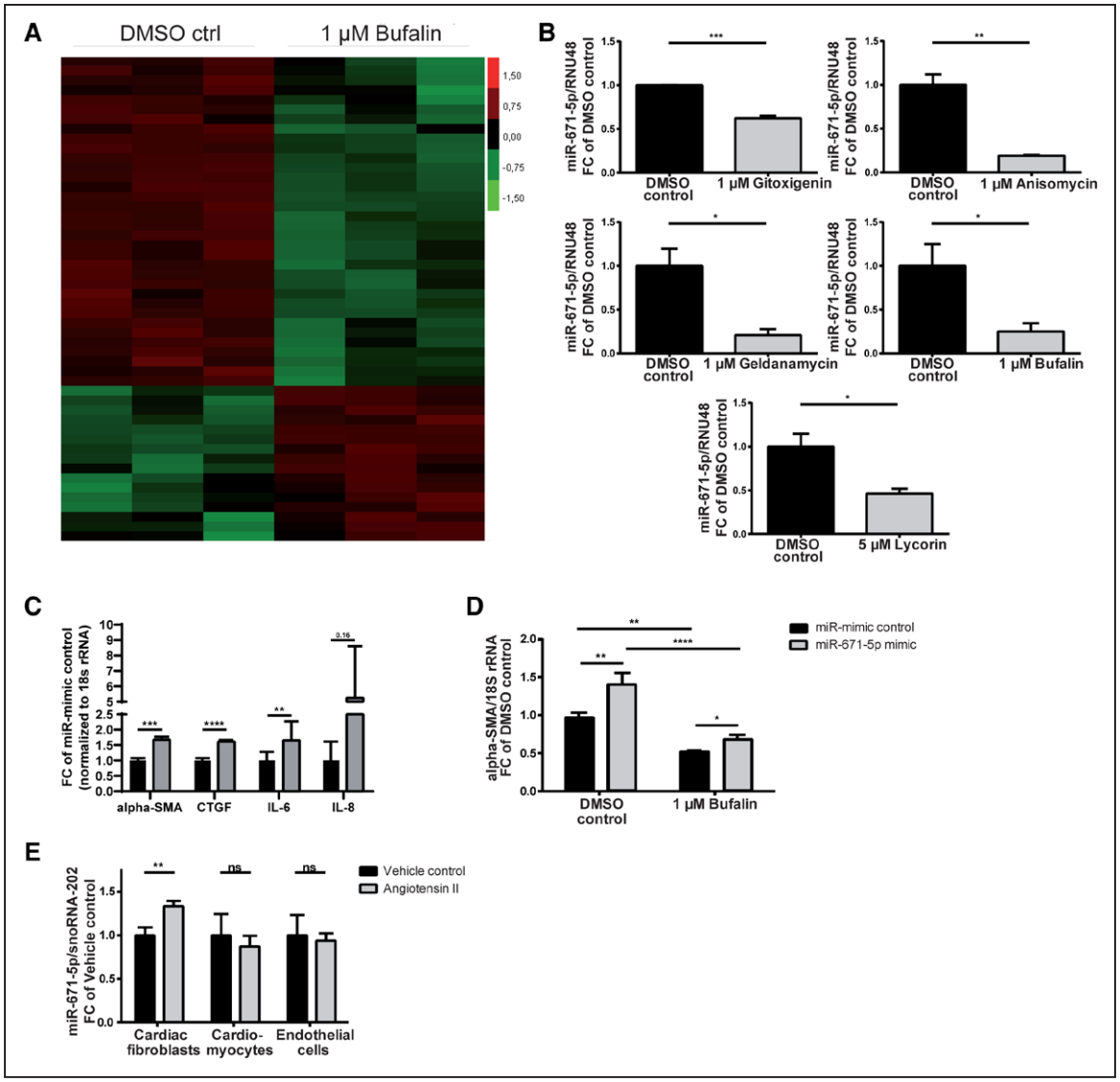

Figure 5. Antifibrotic substances converge on profibrotic microRNA (miR) 671-5p.
A, Representative heat map of differentially regulated miRNAs (unpaired *t* test $P<0.05$) and (**B**) validation of significantly reduced miR-671-5p expression in primary human cardiac fibroblasts (HCFs) on treatment as indicated compared with control (unpaired *t* test, n=3). **C**, Activation of fibrosis markers α-smooth muscle actin (α-SMA), connective tissue growth factor (CTGF), and proinflammatory cytokines interleukin (IL)-6 and IL-8 in primary HCFs after overexpression of miR-671-5p (unpaired *t* test, n=5, miR-mimic control vs miR671-5p mimic). **D**, Restoration of diminished α-SMA expression of primary HCFs after treatment with bufalin by miR-671-5p (2-way ANOVA, Tukey multiple-comparisons test, dimethyl sulfoxide [DMSO] control vs 1 µmol/L bufalin; unpaired *t* test, miR-mimic control vs miR-671-5p mimic; n=5). **E**, MiR-671-5p expression in murine heart cell fractions after infusion with angiotensin II for 2 weeks (unpaired *t* test, n=6/10). All values from **B** through **E** are presented as mean±SEM. RNU48 indicates small-nucleolar RNA48. **P*<0.05, ***P*<0.01, ****P*<0.001, *****P*<0.0001.

mRNA expression was observed with treatment with the compounds bufalin or lycorine alone (Figure 6E). In line with this finding, rescued SEPP1 protein expression reduction by Ang II infusion has been shown in the bufalin-treated group compared with the dimethyl sulfoxide–treated group (Figure VIIH in the online-only Data Supplement). Likewise, this normalization was evident in vitro; bufalin significantly reversed the decline of SEPP1 protein associated with Ang II stimulation of HCFs (Figure VIIG in the online-only Data Supplement). These results might explain the superior efficacy of bufalin both in vitro and in the therapeutic setting at applied doses (Figures 1 and 3). To further establish the mechanistic role of *SEPP1* as a downstream target of miR-671-5p, transcriptional activation of α-SMA in primary HCFs was followed up after siRNA-mediated silencing of *SEPP1* on treatment with bufalin. The bufalin-induced decline of α-SMA expression in primary HCFs was restored by specific silencing of *SEPP1* in primary HCFs via siRNA chemistry (Figure 6F), thereby replicating the impact of repressing *SEPP1* by miR-671-5p overexpression (Figure 5D). Collectively, these results suggest that *SEPP1* might be the antifibrotic target of miR-671-5p, which partly explains the mechanistic involvement of this miRNA in the antifibrotic efficacy of bufalin (Figure 7).

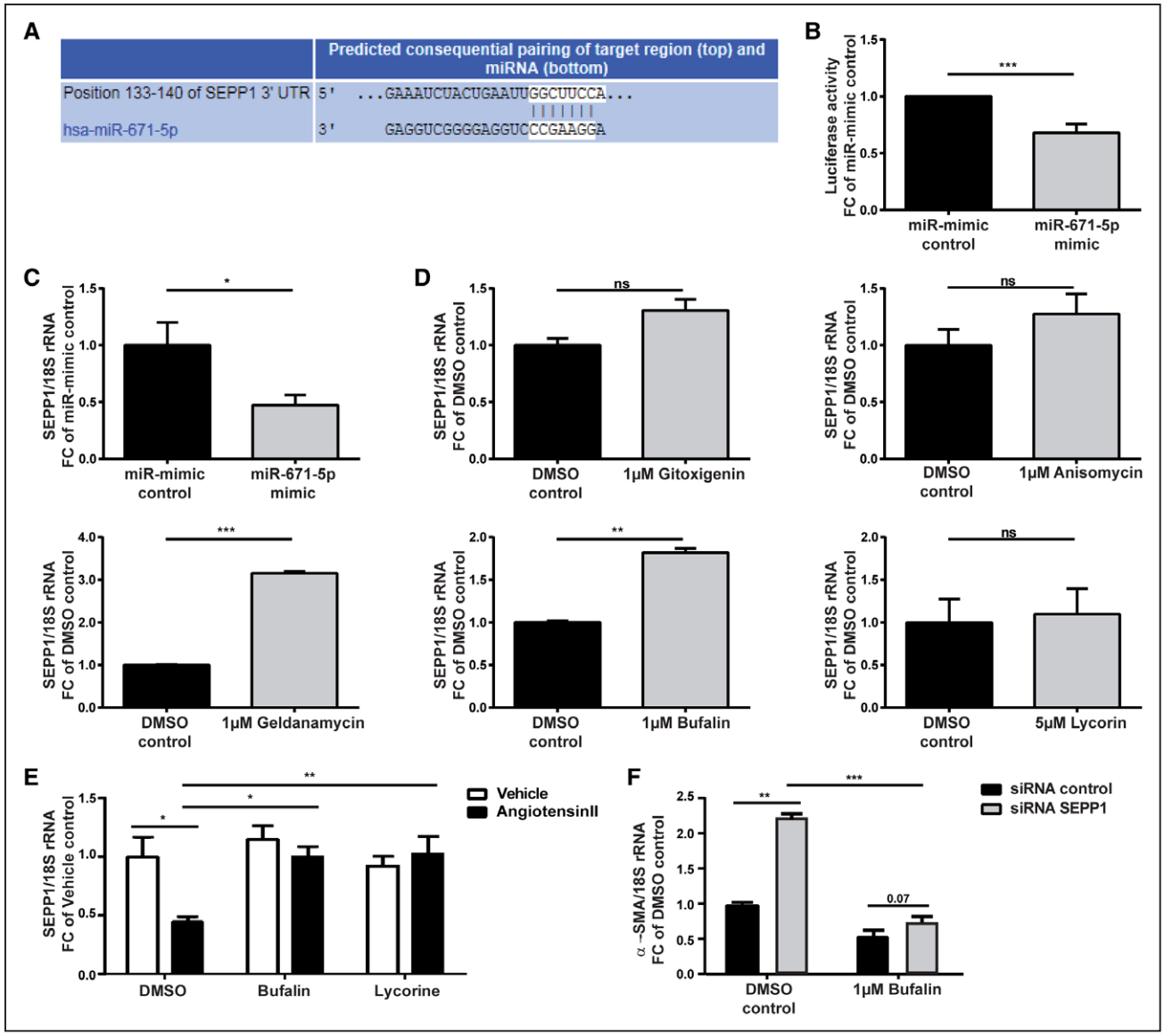

Figure 6. MicroRNA (miR) 671-5p drives fibrosis via repression of selenoprotein P1 (*SEPP1*).
A, Predicted base pairing between the seed sequence of human miR-671-5p and target sequence in the 3′ untranslated region (UTR) of *SEPP1* (TargetScanHuman, version 7.1). **B**, Luciferase activity levels on transfection of a luciferase construct containing the 3′ UTR of *SEPP1* with miR-mimic control or miR-671-5p mimic (1-sample *t* test, n=27 replicates). **C**, Significant reduction of *SEPP1* mRNA levels in primary human cardiac fibroblasts (HCFs) after overexpression of miR-671-5p (unpaired *t* test, n=3). **D**, *SEPP1* levels follow the opposite pattern compared with miR-671-5p in primary HCFs on treatment with the lead antifibrotic substances (unpaired *t* test, n=2-3). **E**, Decrease of *SEPP1* levels in cardiac tissue after 8 weeks of angiotensin II infusion (therapeutic mouse study) is significantly counteracted by bufalin and lycorine (2-way ANOVA, Tukey multiple-comparison test, n=18/8/7/17/18/16). **F**, Restoration of diminished α-SMA expression in primary HCFs after treatment with bufalin by siRNA-mediated silencing of *SEPP1* (2-way ANOVA, Sidak multiple-comparisons test, dimethyl sulfoxide [DMSO] control vs 1 µmol/L bufalin; unpaired *t* test, siRNA control vs siRNA SEPP1; n=4). All values from **C** through **F** are presented as mean±SEM. **P*<0.05, ***P*<0.01, ****P*<0.001.

DISCUSSION

Here, we show the effective antifibrotic potential of the 2 naturally derived compounds bufalin and lycorine both in primary HCFs and in multiple rodent models of cardiac remodeling in preventive and therapeutic settings. Bufalin in particular preserved global and diastolic function of the heart, correlating with a significant reduction of collagen deposition. Moreover, bufalin ameliorated cardiac function when treatment was started at a time point of already established diastolic dysfunction, underscoring its clinical translational importance. Both substances were effectively taken up by the heart on systemic delivery in vivo. Continuous monitoring of blood pressure via telemetry uncovered that neither bufalin nor lycorine shows any antihypertensive action on Ang II infusion, excluding the possibility that bufalin or lycorine confers cardioprotection by reducing elevated blood pressure. When the clinically relevant Dahl salt-sensitive rat model was used, fibrosis and diastolic dysfunction were effectively abolished by bufalin and lycorine. This result highlights the reproducibility of

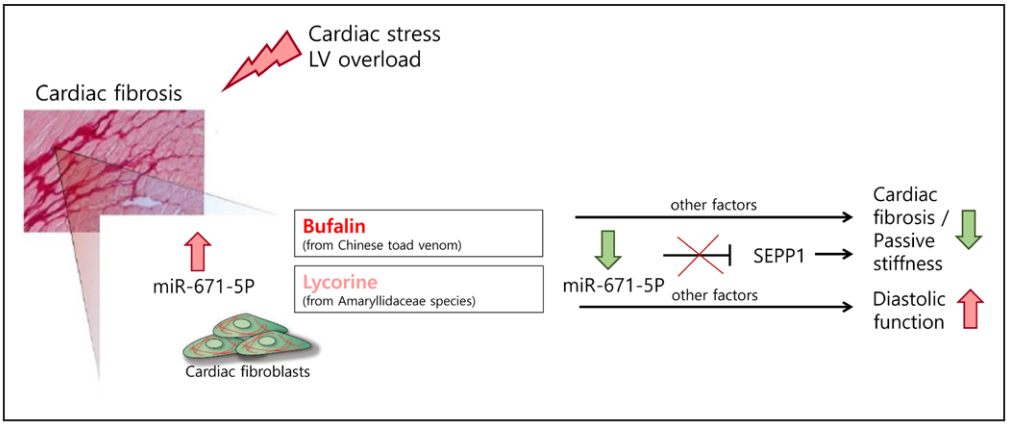

Figure 7. Mechanistic overview.
Proposed therapeutic mode of action for the antifibrotic compounds bufalin and lycorine in angiotensin II–mediated diastolic dysfunction. Treatment with the lead natural compound results in a decline in microRNA (miR) 671-5p levels in cardiac fibroblasts, which, in turn, leads to derepression of its target selenoprotein P1 (*SEPP1*). LV indicates left ventricular.

the antifibrotic effects seen in hypertensive mice in an additional species and model.

The cardioprotective potential of bufalin and lycorine may be attributed to their suppressive effects on proliferation and collagen production of cardiac fibroblasts, the effector cells of fibrosis in the diseased heart. Mechanistically, we identified miR-671-5p as a common key player of the lead candidates mediating fibrosis in primary HCFs. Hence, modulation of miR-671-5p in the heart might be harnessed as an alternative therapeutic strategy for treatment of cardiac fibrotic diseases. However, careful risk analysis would be required because miR-671-5p is ubiquitously expressed in various cell types and organs (Figure VIID in the online-only Data Supplement), which may give rise to unintended off-target effects. In addition, no changes have been shown in fibrosis and inflammatory markers with sole inhibition of miR-671-5p (Figure VIIA in the online-only Data Supplement), whereas significant reductions of miR-671-5p have been seen in natural compound–treated animals (Figure 5C), suggesting that additional mechanisms are involved in the observed antifibrotic effect of the compounds.

We found that profibrotic effects of miR-671-5p might be mediated by repression of its target SEPP1. This protein transports the dietary trace element selenium from the liver to target tissues and was described as part of the antioxidant defense line and an important cardioprotector.[8,26,28,29] Here, we show that *SEPP1* is also a target of miR-671-5p in primary HCFs, which express this protein in remarkably high amounts. Our findings imply an antifibrotic, protective role of SEPP1, possibly preventing myocardial stiffness in vivo. We consistently found expression levels of *SEPP1* to be decreased in fibrotic cardiac tissue of our murine model of diastolic dysfunction caused by prolonged Ang II infusion (therapeutic approach). Bufalin in particular significantly recovered *SEPP1* levels, possibly explaining apparent higher effectivity of this compound in a therapeutic setting.

Despite some efforts to develop new therapeutic approaches for the treatment of patients with HF with diastolic dysfunction and its progression to end-stage systolic HF, the life expectancy of patients remains unacceptably low.[30] Cardiovascular diseases still account for the highest number of deaths worldwide.[3] Myocardial fibrosis is a hallmark of cardiac remodeling and a major determinant for both the development and progression of HF.[2] Thus, a breakthrough discovery for a therapeutic strategy to target primarily maladaptive responses in cardiac fibroblasts would be indispensable. We provide evidence for cardioprotective and antifibrotic effects and the promising safety-tolerability profile of the natural compounds bufalin and lycorine, thereby laying the groundwork for prospective preclinical and clinical studies for both the prevention and treatment of fibrotic cardiac diseases. To date, no promising treatment for patients with diastolic dysfunction exists. Indeed, the understanding of the association between diastolic dysfunction and clinical syndrome of HF is still poor. Therefore, future clinical testing of compounds that show strong cardiac antifibrotic effects and improve diastolic function in selected patients with HF should be explored.

ARTICLE INFORMATION

Received July 11, 2019; accepted December 18, 2019.

The online-only Data Supplement is available with this article at https://www.ahajournals.org/doi/suppl/10.1161/circulationaha.119.042559.

Authors

Katharina Schimmel, PhD*; Mira Jung, PhD*; Ariana Foinquinos, PhD*; Gorka San José, PhD; Javier Beaumont, PhD; Katharina Bock; Lea Grote-Levi; Ke Xiao, PhD; Christian Bär, PhD; Angelika Pfanne; Annette Just; Karina Zimmer; Soeun Ngoy, PhD; Begoña López, PhD; Susana Ravassa, PhD; Sabine Samolovac, PhD; Heike Janssen-Peters, PhD; Janet Remke; Kristian Scherf; Seema Dangwal, PhD; Maria-Teresa Piccoli, PhD; Felix Kleemiss; Fabian Philipp Kreutzer, MSc; Franziska

Kenneweg, PhD; Julia Leonardy, PhD; Lisa Hobuß, MSc; Laura Santer, PhD; Quoc-Tuan Do, PhD; Robert Geffers, PhD; Jan Hinrich Braesen, MD, PhD; Jessica Schmitz, MSc; Christina Brandenberger, PhD; Dominik N. Müller, PhD; Nicola Wilck, MD; Volkhard Kaever, PhD; Heike Bähre, PhD; Sandor Batkai, MD, PhD; Jan Fiedler, PhD; Kevin M. Alexander, MD; Bradley M. Wertheim, MD; Sudeshna Fisch, PhD; Ronglih Liao, PhD; Javier Diez, MD, PhD; Arantxa González, PhD; Thomas Thum, MD, PhD

Correspondence

Thomas Thum, MD, PhD, Institute of Molecular and Translational Therapeutic Strategies (IMTTS), Hannover Medical School, Carl-Neuberg-Strasse 1, 30625 Hannover, Germany. Email thum.thomas@mh-hannover.de

Affiliations

Institute of Molecular and Translational Therapeutic Strategies (K.S., M.J., A.F., K.B., L.G.-L., K.X., C. Bär, A.P., A.J., K.Z., S.S., H.J.-P., J.R., K.S., S.D., M.-T.P., F.K., F.P.K., F.K., J.L., L.H., L.S., S.B., J.F., T.T.), Institute for Pathology, Nephropathology Unit (J.H.B., J.S.), Institute of Functional and Applied Anatomy (C. Brandenberger), Research Core Unit Metabolomics, Institute of Pharmacology (V.K., H.B.), and REBIRTH Center of Translational Regenerative Medicine (T.T.), Hannover Medical School, Germany. Cardiovascular Institute, Stanford University School of Medicine, CA (K.S., S.D., K.M.A., R.L.). Program of Cardiovascular Diseases, CIMA Universidad de Navarra and IdiSNA, Pamplona, Spain (G.S.J., J.B., B.L., S.R., J.D., A.G.). CIBERCV, Institute of Health Carlos III, Madrid, Spain (G.S.J., J.B., B.L., S.R., J.D., A.G.). Department of Medicine, Divisions of Genetics and Cardiology (S.N., S.F., R.L.), and Department of Medicine, Division of Pulmonary and Critical Care Medicine (B.M.W.), Brigham and Women's Hospital, Harvard Medical School, Boston, MA. Greenpharma SAS, Department of Chemoinformatics, Orléans, France (Q.-T.D.). Helmholtz Centre for Infection Research, Research Group Genome Analytics, Braunschweig, Germany (R.G.). Experimental and Clinical Research Center, a cooperation of Charité-Universitätsmedizin Berlin and Max Delbrück Center for Molecular Medicine in the Helmholtz Association, Germany (D.N.M., N.W.). Division of Nephrology and Internal Intensive Care Medicine, Charité-Universitätsmedizin Berlin, Germany (N.W.). Department of Cardiology and Cardiac Surgery and Department of Nephrology, Clínica Universidad de Navarra, Pamplona, Spain (J.D.).

Acknowledgments

The authors thank the Hannover Biomedical Research School and the Integrated Research and Treatment Center Transplantation, Hannover Medical School, Germany, for financial support to L. Grote-Levi and K. Bock. They thank Ellen T. Roche, Department of Mechanical Engineering and Institute for Medical Engineering and Science, Massachusetts Institute of Technology, Cambridge, for generous lending of the Millar catheter for the rat study.

Sources of Funding

The study was supported by grants from the European Union project Fibrotarget (7th Framework Project, to Drs Thum, Diez, and González); the European Union ERANET grant EXPERT and the European Research Council grant Longheart (to Dr Thum); the Instituto de Salud Carlos III (CB16/11/00483 and PI18/01469) and the DZHK (German Centre for Cardiovascular Research), partner site Berlin, Germany, to Drs Wilck and Müller; and the Berlin Institute of Health, Berlin, Germany (to Drs Wilck and Müller).

Disclosures

Drs Schimmel, Do, and Thum have filed a patent on the use of antifibrotic natural compounds. Drs Fiedler and Thum have filed patents on the use of noncoding RNAs in cardiovascular diseases. Dr Thum has licensed patents about the use of noncoding RNAs. Drs Thum and Batkai are founders of and hold shares in Cardior Pharmaceuticals GmbH. The other authors report no conflicts.

REFERENCES

1. Jessup M, Brozena S. Heart failure. *N Engl J Med*. 2003;348:2007-2018. doi: 10.1056/NEJMra021498
2. Kong P, Christia P, Frangogiannis NG. The pathogenesis of cardiac fibrosis. *Cell Mol Life Sci*. 2014;71:549–574. doi: 10.1007/s00018-013-1349-6
3. Braunwald E. Heart failure. *JACC Heart Fail*. 2013;1:1–20. doi: 10.1016/j.jchf.2012.10.002
4. Heymans S, Gonzalez A, Pizard A, Papageorgiou AP, Lopez-Andres N, Jaisser F, Thum T, Zannad F, Diez J. Searching for new mechanisms of myocardial fibrosis with diagnostic and/or therapeutic potential. *Eur J Heart Fail*. 2015;17:764–771. doi: 10.1002/ejhf.312
5. Cao Z, Yu D, Fu S, Zhang G, Pan Y, Bao M, Tu J, Shang B, Guo P, Yang P, et al. Lycorine hydrochloride selectively inhibits human ovarian cancer cell proliferation and tumor neovascularization with very low toxicity. *Toxicol Lett*. 2013;218:174–185. doi: 10.1016/j.toxlet.2013.01.018
6. Chang Y, Zhao Y, Gu W, Cao Y, Wang S, Pang J, Shi Y. Bufalin inhibits the differentiation and proliferation of cancer stem cells derived from primary osteosarcoma cells through Mir-148a. *Cell Physiol Biochem*. 2015;36:1186–1196. doi: 10.1159/000430289
7. Chen S, Jin G, Huang KM, Ma JJ, Wang Q, Ma Y, Tang XZ, Zhou ZJ, Hu ZJ, Wang JY, et al. Lycorine suppresses RANKL-induced osteoclastogenesis in vitro and prevents ovariectomy-induced osteoporosis and titanium particle-induced osteolysis in vivo. *Sci Rep*. 2015;5:12853. doi: 10.1038/srep12853
8. Han KQ, Huang G, Gu W, Su YH, Huang XQ, Ling CQ. Anti-tumor activities and apoptosis-regulated mechanisms of bufalin on the orthotopic transplantation tumor model of human hepatocellular carcinoma in nude mice. *World J Gastroenterol*. 2007;13:3374–3379. doi: 10.3748/wjg.v13.i24.3374
9. Hu M, Peng S, He Y, Qin M, Cong X, Xing Y, Liu M, Yi Z. Lycorine is a novel inhibitor of the growth and metastasis of hormone-refractory prostate cancer. *Oncotarget*. 2015;6:15348–15361. doi: 10.18632/oncotarget.3610
10. Jiang L, Zhao MN, Liu TY, Wu XS, Weng H, Ding Q, Shu YJ, Bao RF, Li ML, Mu JS, et al. Bufalin induces cell cycle arrest and apoptosis in gallbladder carcinoma cells. *Tumour Biol*. 2014;35:10931–10941. doi: 10.1007/s13277-014-1911-3
11. Li L, Dai HJ, Ye M, Wang SL, Xiao XJ, Zheng J, Chen HY, Luo YH, Liu J. Lycorine induces cell-cycle arrest in the G0/G1 phase in K562 cells via HDAC inhibition. *Cancer Cell Int*. 2012;12:49. doi: 10.1186/1475-2867-12-49
12. Liu J, Hu JL, Shi BW, He Y, Hu WX. Up-regulation of p21 and TNF-alpha is mediated in lycorine-induced death of HL-60 cells. *Cancer Cell Int*. 2010;10:25. doi: 10.1186/1475-2867-10-25
13. Wu SH, Hsiao YT, Chen JC, Lin JH, Hsu SC, Hsia TC, Yang ST, Hsu WH, Chung JG. Bufalin alters gene expressions associated DNA damage, cell cycle, and apoptosis in human lung cancer NCI-H460 cells in vitro. *Molecules (Basel, Switzerland)*. 2014;19:6047–6057. doi: 10.3390/molecules19056047
14. Xu Y, Chen M, Jin XF, Qian C, Xu XM, Zhang X. Research progress of in vitro and in vivo anti-tumor effects and formulation of bufalin. *Zhongguo Zhong Yao Za Zhi*. 2014;39:2829–2833.
15. Zhao H, Zhao D, Tan G, Liu Y, Zhuang L, Liu T. Bufalin promotes apoptosis of gastric cancer by down-regulation of miR-298 targeting bax. *Int J Clin Exp Med*. 2015;8:3420–3428.
16. Zhao L, Liu S, Che X, Hou K, Ma Y, Li C, Wen T, Fan Y, Hu X, Liu Y, et al. Bufalin inhibits TGF-beta-induced epithelial-to-mesenchymal transition and migration in human lung cancer A549 cells by downregulating TGF-beta receptors. *Int J Mol Med*. 2015;36:645–652. doi: 10.3892/ijmm.2015.2268
17. Chang YW, Zhao YF, Cao YL, Gu W, Pang J, Zhan HS. Bufalin exerts inhibitory effects on IL-1beta-mediated proliferation and induces apoptosis in human rheumatoid arthritis fibroblast-like synoviocytes. *Inflammation*. 2014;37:1552–1559. doi: 10.1007/s10753-014-9882-5
18. Cortes N, Posada-Duque RA, Alvarez R, Alzate F, Berkov S, Cardona-Gomez GP, Osorio E. Neuroprotective activity and acetylcholinesterase inhibition of five *Amaryllidaceae* species: a comparative study. *Life Sci*. 2015:122:42–50. doi: 10.1016/j.lfs.2014.12.011
19. Kang J, Zhang Y, Cao X, Fan J, Li G, Wang Q, Diao Y, Zhao Z, Luo L, Yin Z. Lycorine inhibits lipopolysaccharide-induced iNOS and COX-2 up-regulation in RAW264.7 cells through suppressing P38 and STATs activation and increases the survival rate of mice after LPS challenge. *Int Immunopharmacol*. 2012;12:249–256. doi: 10.1016/j.intimp.2011.11.018
20. Shen JW, Ruan Y, Ren W, Ma BJ, Wang XL, Zheng CF. Lycorine: a potential broad-spectrum agent against crop pathogenic fungi. *J Microbiol Biotechnol*. 2014;24:354–358. doi: 10.4014/jmb.1310.10063
21. Rong X, Ni W, Liu Y, Wen J, Qian C, Sun L, Wang J. Bufalin, a bioactive component of the Chinese medicine chansu, inhibits inflammation and invasion of human rheumatoid arthritis fibroblast-like synoviocytes. *Inflammation*. 2014;37:1050–1058. doi: 10.1007/s10753-014-9828-y

22. Fischer M, Baessler A, Schunkert H. Renin angiotensin system and gender differences in the cardiovascular system. *Cardiovasc Res*. 2002;53:672–677. doi: 10.1016/S0008-6363(01)00479-5
23. Yang XP, Reckelhoff JF. Estrogen, hormonal replacement therapy and cardiovascular disease. *Curr Opin Nephrol Hypertens*. 2011;20:133–138. doi: 10.1097/MNH.0b013e3283431921
24. Leite-Moreira AF. Current perspectives in diastolic dysfunction and diastolic heart failure. *Heart*. 2006;92:712–718. doi: 10.1136/hrt.2005.062950
25. Conceicao G, Heinonen I, Lourenco AP, Duncker DJ, Falcao-Pires I. Animal models of heart failure with preserved ejection fraction. *Neth Heart J*. 2016;24:275–286. doi: 10.1007/s12471-016-0815-9
26. Ayaz M, Turan B. Selenium prevents diabetes-induced alterations in [Zn2+]i and metallothionein level of rat heart via restoration of cell redox cycle. *Am J Physiol Heart Circ Physiol*. 2006;290:H1071–H1080. doi: 10.1152/ajpheart.00754.2005
27. Gharipour M, Sadeghi M, Salehi M, Behmanesh M, Khosravi E, Dianatkhah M, Haghjoo Javanmard S, Razavi R, Gharipour A. Association of expression of selenoprotein P in mRNA and protein levels with metabolic syndrome in subjects with cardiovascular disease: results of the Selenegene study. *J Gene Med*. 2017;19:e2945. 10.1002/jgm.2945. doi: 10.1002/jgm.2945
28. Rose AH, Hoffmann PR. Selenoproteins and cardiovascular stress. *Thromb Haemost*. 2015;113:494–504. doi: 10.1160/TH14-07-0603
29. Saito Y, Hayashi T, Tanaka A, Watanabe Y, Suzuki M, Saito E, Takahashi K. Selenoprotein P in human plasma as an extracellular phospholipid hydroperoxide glutathione peroxidase: isolation and enzymatic characterization of human selenoprotein p. *J Biol Chem*. 1999;274:2866–2871. doi: 10.1074/jbc.274.5.2866
30. Ferrari R, Bohm M, Cleland JG, Paulus WJ, Pieske B, Rapezzi C, Tavazzi L. Heart failure with preserved ejection fraction: uncertainties and dilemmas. *Eur J Heart Fail*. 2015;17:665–671. doi: 10.1002/ejhf.304